Ising metamagnets in thin film geometry: Equilibrium properties

Yen-Liang Chou and Michel Pleimling
Department of Physics, Virginia Tech, Blacksburg, Virginia 24061-0435, USA
(Received 12 July 2011; published 17 October 2011)

Artificial antiferromagnets and synthetic metamagnets have attracted much attention recently due to their potential for many different applications. Under some simplifying assumptions, these systems can be modeled by thin Ising metamagnetic films. In this paper we study, using both the Wang-Landau scheme and importance sampling Monte Carlo simulations, the equilibrium properties of these films. On the one hand, we discuss the microcanonical density of states and its prominent features. On the other hand, we analyze canonically various global and layer quantities. We obtain the phase diagram of thin Ising metamagnets as a function of temperature and external magnetic field. Whereas the phase diagram of the bulk system exhibits only one phase transition between the antiferromagnetic and paramagnetic phases, the phase diagram of thin Ising metamagnets includes an additional intermediate phase where one of the surface layers has aligned itself with the direction of the applied magnetic field. This additional phase transition is discontinuous and ends in a critical end point. Consequently, it is possible to gradually go from the antiferromagnetic phase to the intermediate phase without passing through a phase transition.

DOI: 10.1103/PhysRevB.84.134422 PACS number(s): 75.10.Hk, 75.30.Kz, 75.70.−i, 75.40.Mg

I. INTRODUCTION

Artificial antiferromagnets, formed of nanostructured superlattices that are coupled antiferromagnetically, have been the focus of many recent studies, due to their high potential for innovative technological applications. These possible applications range from high-density recording technology[1] to spintronics devices[2] and magnetic refrigeration.[3] Artificial antiferromagnets are heterostructures composed of ferromagnetic layers that are coupled antiferromagnetically via spacers. This structure yields a high level of control over both the intra- and interlayer interactions, allowing for a tailoring of the physical properties. Examples include [Co/Pt]/Ru, where ferromagnetic Co/Pt multilayers are periodically separated by Ru layers,[4,5] or Co/Cr, where thin Co films are separated by the spacer Cr.[3] The magnetic moments of the ferromagnetic layers can thereby be either perpendicular (as is the case for Co/Pt with perpendicular anisotropy) or parallel (as encountered in Co films) to the interface separating the ferromagnetic layers from the spacers.

[Co/Pt]/Ru, with strong perpendicular anisotropy, as well as the related systems like [Co/Pt]/NiO, Co/Ir, and Fe/Au, have been called synthetic metamagnets,[6] as they can exhibit a regime with an antiferromagnetic phase at low external magnetic fields and a paramagnetic phase at large fields. When the value of the magnetic field is changed, plateaus show up in the magnetic hysteresis of these films, due to the fact that different layers reverse their magnetization at different values of the field.[4] In fact, for an even number of identical ferromagnetic layers in a thin film, exactly two metamagnetic transitions are observed, as one of the outermost layers switches at a lower field than the internal layers.[6] The same sequence of phases should also be realized for in-plane magnetization and strong anisotropy.[7]

In a phenomenological approach it is customary in systems with strong perpendicular anisotropy to replace the ferromagnetic multilayers by a single ferromagnetic layer.[6,7] This naturally leads to a modeling of synthetic metamagnets by an Ising metamagnet, i.e., a layered Ising model with ferromagnetic in-layer interactions and antiferromagetic interactions between adjacent layers. The advantage of using a layered Ising model is that this type of model is perfectly suited for a study of thermal properties through standard numerical methods. However, modeling ferromagnetic multilayers by single ferromagnetic layers also has its restrictions as it does not allow a theoretical description of the multidomain states, composed of metamagnetic stripe and bubble domains, that may form when a magnetic field is applied to an artificial antiferromagnet with strong anisotropy.[5,8]

Over the years Ising metamagnets have attracted quite some attention on their own.[9–30] Indeed, due to their simplicity, Ising metamagnets are ideal systems to study the properties of a tricritical point that separates a discontinuous transition between the antiferromagnetic and paramagnetic phases at high fields and low temperatures from a continuous transition between the same phases at low fields and high temperatures. In addition, the mean-field prediction of a decomposition of the tricritical point into a critical end point and a double critical end point[10] has led to systematic numerical investigations of this possible scenario. Whereas many studies have concluded that this decomposition does not take place in short-range models,[13,14,22,23] the increase of the interlayer coordination, which brings the model closer to being of mean-field type, yields anomalies in the specific heat and the magnetization[17,19] that resemble those measured in $FeBr_2$.[31,32]

The general behavior of Ising metamagnets is by now well understood. However, all mentioned studies focused on bulk systems and no systematic studies of metamagnetic properties of thin Ising films have been done to our knowledge. The recent interest in synthetic metamagnets warrants an in-depth understanding of metamagnets in confined geometries, and we propose here a step in that direction by studying thin Ising metamagnetic films.

An additional motivation for our work comes from the recent analysis[33] of nonequilibrium relaxation processes in Co/Cr superlattices. This study revealed that intriguing aging phenomena take place in layered antiferromagnets. In order

to better understand these observations a thorough study of the dynamical properties of related theoretical models is needed. However, before being able to study in depth the nonequilibrium properties of metamagnetic films, we found it necessary to first fully understand the equilibrium properties of these systems. Therefore we focus in this paper on the equilibrium phase diagram of thin metamagnetic films. The nonequilibrium properties of these systems will be discussed in a separate presentation.

Our paper is organized in the following way. After having introduced our model in Sec. II, we discuss in Sec. III its equilibrium properties. Using the Wang-Landau scheme, we determine the density of states (degeneracy) of our classical model and discuss its prominent features. This density of states is then used for a canonical analysis of the system, where the focus is on the two phase transitions that are observed in thin film geometry when the external magnetic field is increased. As the Wang-Landau scheme is restricted to small systems, we supplement our study by standard Monte Carlo simulations of larger systems. From these numerical data, we derive the phase diagram of thin metamagnetic films and show that in thin films an additional phase transition line shows up that separates two ordered phases. This transition, which is absent in bulk systems, is found to be discontinuous and to end in a critical end point. Finally, in Sec. IV we discuss our results and conclude.

II. MODEL AND METHODS

We consider a layered lattice model on a cubic lattice where every lattice point i is characterized by an Ising spin $S_i = \pm 1$. The interactions between nearest-neighbor spins are ferromagnetic in the planes perpendicular to the z axis. These two-dimensional planes are coupled antiferromagnetically in the z direction. Adding an external magnetic field of strength B, the Hamiltonian of our system is then given by

$$\mathcal{H} = -J_{xy} \sum_{\langle i,j \rangle} S_i S_j + J_z \sum_{(i,j)} S_i S_j - B \sum_i S_i = E - BM, \tag{1}$$

where we have introduced the internal energy $E = -J_{xy} \sum_{\langle i,j \rangle} S_i S_j + J_z \sum_{(i,j)} S_i S_j$ and the magnetization $M = \sum_i S_i$. The sums over $\langle i,j \rangle$ $[(i,j)]$ are sums over nearest-neighbor pairs in the plane [along the z direction]. The intralayer and interlayer coupling strengths are given by $J_{xy} > 0$ and $J_z > 0$.

In contrast to previous studies, we focus on thin films which are realized by imposing free boundary conditions in the z direction, whereas in the x and y directions we have periodic boundary conditions. In accordance with the synthetic metamagnets, we consider rather few layers, typically $L = 8$ or 10 (we restrict ourselves to even numbers of layers). For the case of periodic boundary conditions in all three directions, which has been studied extensively in the past, the system undergoes a metamagnetic transition between an antiferromagnetic phase and a paramagnetic phase when the field strength is increased. This transition is discontinuous for high fields and low temperatures and continuous for low fields and high temperatures. It is expected that an additional transition shows up when films are considered, this transition being characterized by the alignment of the magnetization of one of the outermost planes with the external field.[4,6]

We study this system using different simulation techniques. In order to elucidate its static properties we compute the degeneracy (or density of states) $\Omega(E,M)$ as a function of internal energy E and magnetization M using the Wang-Landau scheme.[34,35] The degeneracy can then be used for a standard canonical analysis, with the partition sum as a function of temperature T and magnetic field B being given by (we choose units for which $k_B = 1$)

$$Z(T,B) = \sum_E \sum_M \Omega(E,M) e^{-E/T + BM/T}. \tag{2}$$

All global quantities of interest (like the mean magnetization, the mean energy, the susceptibility, and the specific heat) then follow from derivatives of Z with respect to T and B. It is well known that the Wang-Landau scheme usually yields a very good estimate for the degeneracy, allowing for a detailed canonical analysis. However, only rather small systems can be studied in this way. We therefore supplement our study with traditional importance sampling simulations of larger system sizes, using the Metropolis algorithm. We thereby study thin films with layers that contain $L \times L$ spins, with $L = 8$, 16, 32, and 64. Relevant quantities are computed for a large number of temperatures and field strengths; in order to completely cover the phase diagram, the increment between successive T and B values is typically 0.01.

III. EQUILIBRIUM PROPERTIES

We focus in the following on the thermal equilibrium properties of thin Ising ferromagnets. The statistical physics treatment of our classical spin models allows for an in-depth discussion of its properties as a function of all relevant parameters, which in our case are the temperature and the strength of the magnetic field.

A. The density of states

As already mentioned, we compute for our smaller systems the density of states $\Omega(E,M)$, i.e., the number of microscopic configurations that have the same internal energy E and the same magnetization M. Having this two-dimensional histogram at our disposal, we can then compute all relevant global thermodynamic quantities from the partition sum (2) and its derivatives by simply inserting the numerical values for T and B.

Before doing that we briefly discuss the density of states itself. Figure 1 shows the microcanonical entropy $S(E,M) = \ln \Omega(E,M)$ as a function of the energy density $e = E/N$ and the magnetization density $m = M/N$ (here N is the total number of spins in our systems) for three different cases. Whereas in Fig. 1(a) we consider a system with periodic boundary conditions composed of $N = 8 \times 8 \times 8$ spins, with $J_{xy} = J_z$, in Figs. 1(b) and 1(c) we show two systems of $N = 8 \times 8 \times 8$ sites with free boundary conditions in the z direction, the different systems having different relative strengths of the interactions: $J_{xy} = J_z$ in (b) and $J_{xy} = 2J_z$ in (c).

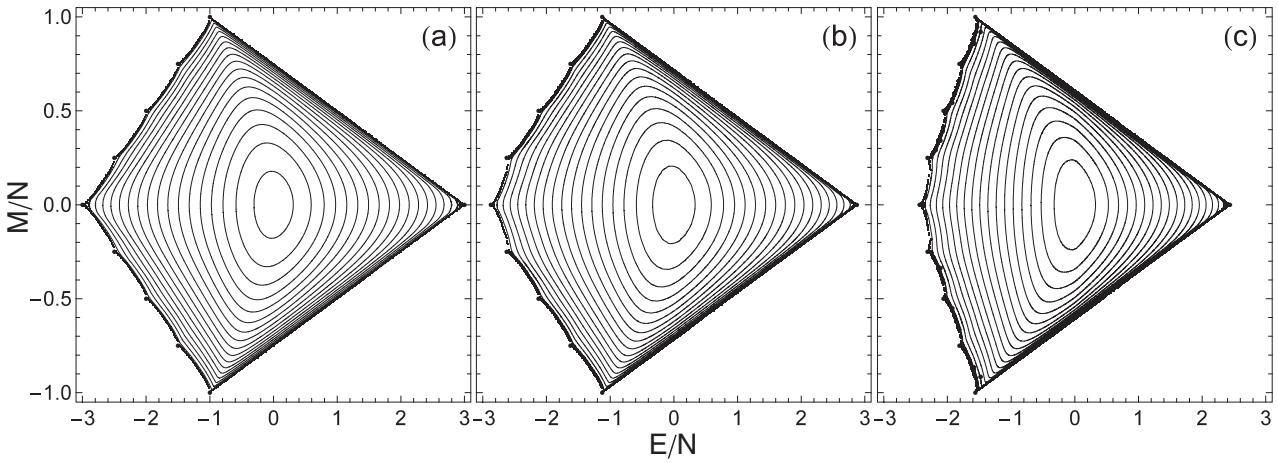

FIG. 1. Microcanonical entropy $S(e,m)$ as a function of energy density $e = E/N$ and magnetization density $m = M/N$ for systems containing $N = 8 \times 8 \times 8$ spins. (a) Periodic boundary conditions in all three directions and $J_{xy} = J_z$, (b) free surfaces in the z direction with $J_{xy} = J_z$, and (c) free surfaces in the z direction with $J_{xy} = 2J_z$. The increment between two successive contour lines is 20. The supports of the entropy surfaces are indicated by the larger points.

In a microcanonical analysis one infers physical properties of a system from a direct study of the microcanonical entropy $S(e,m)$.[36,37] Most investigations of this type focus on spin models with ferromagnetic nearest-neighbor interactions, as for example the standard Ising or Potts models,[38–46] or on polymer models.[47,48] Due to its complicated interactions, the microcanonical entropy of the Ising metamagnet is more complex than, for example, that of the standard nearest-neighbor Ising model;[37] see Fig. 1. Still, some of its features and properties are readily understood.

First, there are obvious properties that are independent of the boundary conditions and of the interaction ratio J_z/J_{xy}. The ground state is twofold degenerate and has magnetization zero (recall that we study only systems with even numbers of layers), with the fully ordered layers pointing alternatively in the up or down direction. Obviously, a given ground state can be changed into the other ground state by multiplying all the spins by -1. This symmetry of the internal energy also shows up in the symmetry of the entropy surfaces with respect to the $M = 0$ line. Interestingly, the entropy surfaces all display prominent kinks at magnetizations $M/N = \pm 2\mu/L$, with $\mu = 0, \ldots, L/2$, corresponding to configurations with fully ordered planes where μ planes have been flipped with respect to the ground state.

A change in the interaction ratio J_z/J_{xy} [see Figs. 1(b) and 1(c)] mainly changes the range of accessible energies. As a result, smaller values of J_z/J_{xy} yield a compressed, but otherwise unchanged, entropy surface.

At a first look, changing the boundary condition in the z direction also seems to have only minor effects on $s(e,m)$. However, one notes that the energy difference between the ground state and the state with one flipped layer, with $M/N = \pm 2/L = \pm 1/4$ in Fig. 1, is smaller for the free boundaries in the z direction than for the periodic boundaries; compare Figs. 1(a) and 1(b). As we already argued in the Introduction (and as we will see later in the canonical analysis), our metamagnetic films should display two metamagnetic transitions, a first transition at low magnetic fields, where only one surface layer is flipped, and a second transition at higher fields, where the remaining layers pointing opposite to the magnetic field are flipped. In contrast, a system with periodic boundary conditions in all three directions is known to undergo a single metamagnetic transition.[10] With this in mind, it seems surprising that very similar-looking entropy surfaces should yield these different phase transition sequences.

In fact, it is the decrease of the energy difference between the ground state and the states with fully ordered planes and magnetization $M/N = \pm 2/L$ that ultimately is responsible for the emergence of this additional transition. We show that in Fig. 2, where we plot for systems with $J_z = J_{xy}$ the quantity $(E - BM - TS)/N$ as a function of M/N, with $T = 1$ and different values of B. In the canonical ensemble, the corresponding quantity is of course the Helmholtz free-energy density, which is minimal for the stable state. But even without making a canonical average one can read off the stable phase from the "microcanonical" quantity plotted in Fig. 2. For the system with periodic boundary conditions [see Fig. 2(a)], our quantity is minimal for $M = 0$ and low fields. When the field strength exceeds $B = 2$, a metamagnetic phase transition takes place such that the stable phase is now the paramagnetic phase with $M/N = 1$. Conversely, for the thin film geometry [see Fig. 2(b)], a first transition to a phase with one flipped layer and magnetization $M/N = 2/L = 1/4$ shows up at $B = 1$, as can be seen when studying the global minimum of $E - BM - TS$, followed by a second discontinuous transition at $B = 2$. In this way, the sequence of phase transitions can indeed be unraveled in a microcanonical analysis.

B. Thermal quantities

Even though the microcanonical analysis allows determination of the sequence of phases, an in-depth study of the thermal properties of the metamagnetic films warrants a canonical analysis of the standard quantities as a function of temperature and magnetic field. In the following, we discuss small systems for which the density of states can be obtained numerically,

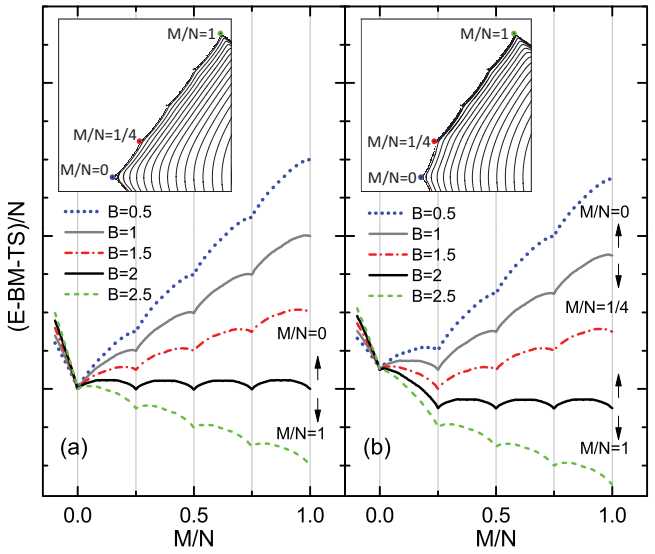

FIG. 2. (Color online) Microcanonical quantity $(E - BM - TS)/N$ as a function of M/N. The canonical correspondence of this quantity is the Helmholtz free-energy density. The global minimum of the plotted quantity allows us to understand the sequence of phases that show up when the strength of the magnetic field is changed. The systems contain $N = 8 \times 8 \times 8$ spins, with (a) periodic boundary conditions and (b) free boundary conditions in the z direction. The insets show the relevant parts of the microcanonical entropy; see the main text.

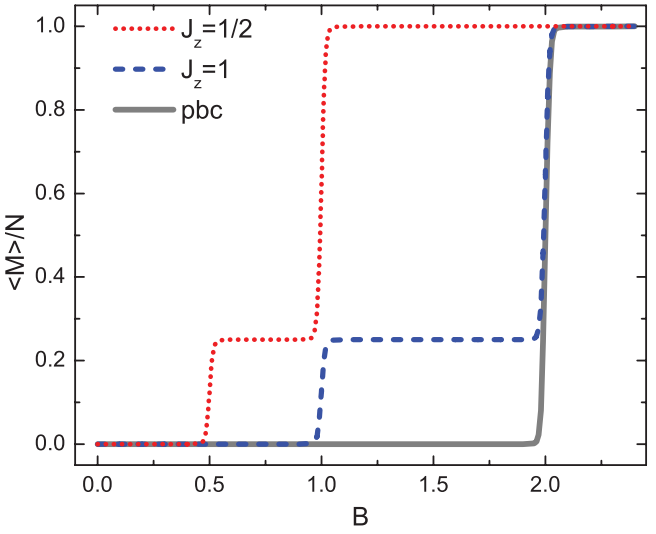

FIG. 3. (Color online) Average magnetization as a function of magnetic field strength B at temperature $T = 1$. The magnetization is shown for thin metamagnetic films with different interaction ratios as well as for a sample with periodic boundary conditions (pbc) and $J_z = 1$. The three-dimensional samples contain $N = 8^3$ spins, with the interlayer interaction having the strength $J_{xy} = 1$.

as discussed in the previous section. This density of states $\Omega(E,M) = e^{S(E,M)}$ is then used for the computation of the partition sum and related quantities. Thus, for a quantity $Q(E,M)$ the thermal average at temperature T and field strength B is

$$\langle Q\rangle = \sum_E \sum_M Q(E,M)\Omega(E,M)e^{-(E-BM)/T}/Z(T,B), \quad (3)$$

where the partition function $Z(T,B)$ is given by Eq. (2). In order to elucidate the thermal properties of thin metamagnets we studied the average magnetization $\langle M\rangle$, the average energy $\langle E\rangle$, the magnetic susceptibility $\chi = \frac{1}{NT}[\langle M^2\rangle - \langle M\rangle^2]$, and the specific heat $C = \frac{1}{NT^2}[\langle \mathcal{H}^2\rangle - \langle \mathcal{H}\rangle^2]$.

We supplement this canonical analysis of small systems based on the density of states by standard canonical simulations of larger systems, with the same number of layers but different numbers of spins in the layers. This allows us to assess the finite-size effects and to extrapolate to films with a large number of spins in every layer. Standard importance sampling Monte Carlo simulations often yield results of lesser quality than the canonical analysis based on the Wang-Landau scheme. On the other hand, larger systems can easily be simulated. In addition, we also can look at additional quantities which are not accessible when we start from the degeneracy as a function of total magnetization and total energy. Thus we will also study the layer susceptibility

$$\chi(z) = \frac{1}{L^2T}[\langle M^2(z)\rangle - \langle M(z)\rangle^2], \quad (4)$$

where $M(z)$ is the magnetization of layer z. Of special interest is of course the susceptibility $\chi(1)$ of the layer $z = 1$ that flips in the direction of the magnetic field when the low-field phase transition line is crossed. Similarly, we also study the layer specific heat

$$C(z) = \frac{1}{L^2T^2}[\langle \mathcal{H}^2(z)\rangle - \langle \mathcal{H}(z)\rangle^2], \quad (5)$$

where $\mathcal{H}(z) = -J_{xy}\sum_{\langle i,j\rangle_z} S_iS_j - B\sum_i^{\text{layer } z} S_i$ is the in-layer contribution to the energy in layer z.

Figure 3 highlights the expected difference in the field dependence of the magnetization between thin films and bulk systems (i.e., systems with periodic boundary conditions). For thin films a first transition takes place for $B \approx J_z$, where one of the outer layers completely flips, followed by a second transition at $B \approx 2J_z$, where the remaining layers align with the magnetic field. At $T = 0$ these transitions take place exactly at $B = J_z$ and $B = 2J_z$. For larger T than that used in Fig. 3, the total magnetization after the flipping of the outer layer is slightly lower than $N/4$, due to thermal fluctuations.

We discuss the T and B dependence of our thermal quantities in Fig. 4 for a thin film of eight layers with $J_z = J_{xy} = 1$. The two phase transitions are readily seen in the changes of the magnetization density [plateaus in Fig. 4(c)] and the susceptibility [lines of maxima in Fig. 4(d)]. One notes that for small T the change in the magnetization is very abrupt, pointing to a discontinuous transition, whereas for larger T this change is much more gradual, in agreement with a continuous transition. This change of the nature of the transition also shows up in the susceptibility. Two lines of maxima, one being hardly visible on the scale of the figure, are also observed in the specific heat [see Fig. 4(b)].

Based on the positions of the maxima in the response functions (see Figs. 6, 7, and 8 below), we obtain the phase diagram for a thin metamagnetic film composed of eight layers shown in Fig. 5. We first note the expected presence of three different phases: the paramagnetic phase

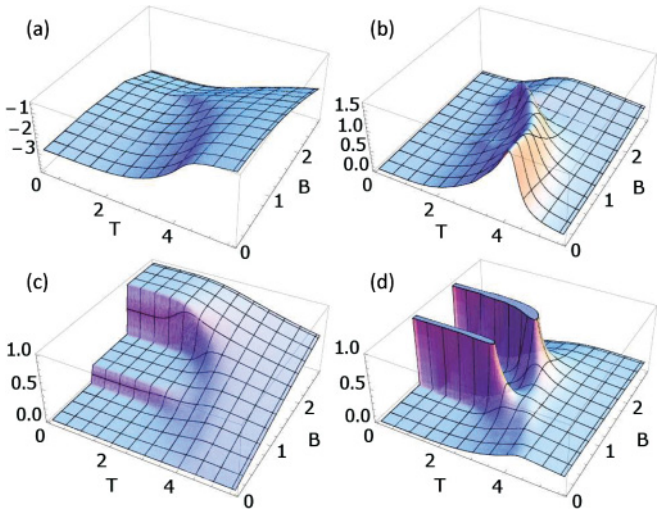

FIG. 4. (Color online) (a) Energy density, (b) specific heat, (c) magnetization density, and (d) susceptibility as functions of T and B for a thin film composed of $N = 8^3$ spins, with $J_z = J_{xy} = 1$.

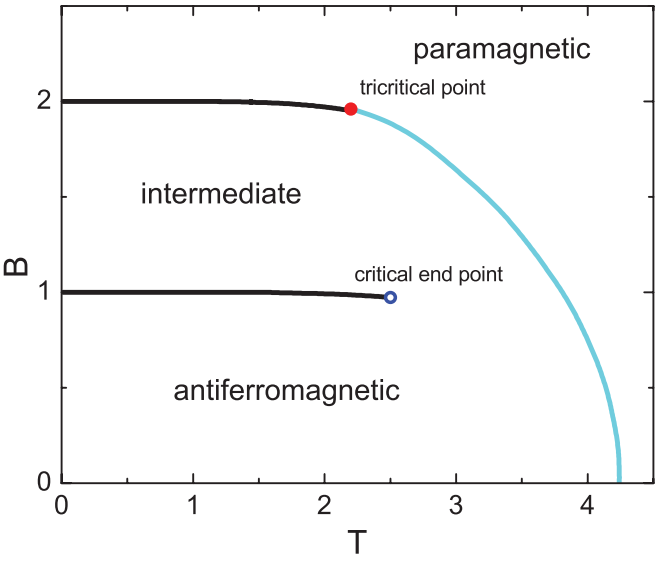

FIG. 5. (Color online) Phase diagram for the thin Ising metamagnet film with eight layers. The different transition lines result from the maxima of the (global and layer) susceptibility and specific heat. Black lines indicate a discontinuous transition, whereas the continuous transition is shown as a gray (cyan online) line. We observe a tricritical point (filled point) as well as a critical end point (open point).

at high temperatures and high fields, the antiferromagnetic phase at low temperatures and low fields, and a phase which has a nonzero magnetization at intermediate fields and low temperatures. Similar to what is observed in the phase diagram of the bulk system, the transition between the ordered and paramagnetic phases is discontinuous at low temperatures and continuous at high temperatures, with a tricritical point separating these two regimes. We locate this point at $T = 2.20(1)$ and $B = 1.96(1)$. At low temperatures the transition between the antiferromagnetic phase and the intermediate phase is also discontinuous. This transition, however, does not extend all the way up to the phase transition line separating the ordered phase from the paramagnetic phase, but instead ends at a critical end point located at $T = 2.50(5)$ and $B = 0.98(1)$; see below.

Increasing the thickness of the film leaves the phase diagram qualitatively unchanged. A slight shift in the phase transition lines, especially at high temperatures and low fields, is observed when the number of layers in the film is changed. This shift of the critical temperature of a film as a function of thickness is of course expected and has been studied extensively, both theoretically and experimentally, in the absence of external magnetic fields (see, for example, Refs. 49–53).

In Figs. 6, 7, and 8 we have a closer look at the different response functions used for the construction of the phase diagram. At low temperatures see [Fig. 6(a)], the peaks in the susceptibility as a function of the magnetic field strength are very pronounced and sharp, indicating the discontinuous character of the transitions. The form of the peaks changes around $T = 2.2$, as here the order of the transition changes from discontinuous to continuous. Above $T = 2.2$ [see Fig. 6(c)], the height of the peaks shows the expected size dependence of a continuous transition. Figure 6(d) shows the total susceptibility at the rather high temperature of $T = 3.5$. Increase in the system size reveals the emergence of a critical peak at $B \approx 1.3$. This peak, which coincides which the transition to the paramagnetic phase, shows up only as a shoulder in the smaller systems. The additional peak at $B \approx 1.6$ is a noncritical one and is similar to that observed in the bulk system.

Another way to monitor the phase transition lines is through a study of the specific heat as a function of temperature. As an example, Fig. 7(a) shows the specific heat for vanishing magnetic field. Only one critical peak is observed, which results from the phase transition between the ordered low-temperature phase and the disordered high-temperature phase. In Fig. 7(b) we show the field dependence of the maximum of the specific heat along the phase transition line to the paramagnetic phase. For low fields this transition is continuous, and the specific heat height shows the expected finite-size scaling of an ordinary critical point. For a fixed system size, the specific heat exhibits a strong peak around $B \approx 1.96$ which is due to the change of the order of the phase transition when the tricritical point is crossed.

The standard way to locate the tricritical point is to monitor the hysteresis observed when the phase transition line is crossed at low fields,[14,23] as the hysteresis loop vanishes when the tricritical point is approached. We found it useful to monitor in addition the location of a noncritical high-field peak observed for temperatures larger than the temperature of the tricritical point. This noncritical peak is also observed in metamagnetic bulk systems, both in simulations[20] and in experiments.[54] The merging of this noncritical line with the phase transition line separating the paramagnetic phase from the ordered phases allows a reliable estimation of the location of the tricritical point. Another estimate can be obtained by monitoring the strong increase of the peak heights of response functions when the tricritical point is approached, as shown in Fig. 7(b). Taking all this into account, we estimate the tricritical point of our thin film to be at $T = 2.20(1)$ and $B = 1.96(1)$.

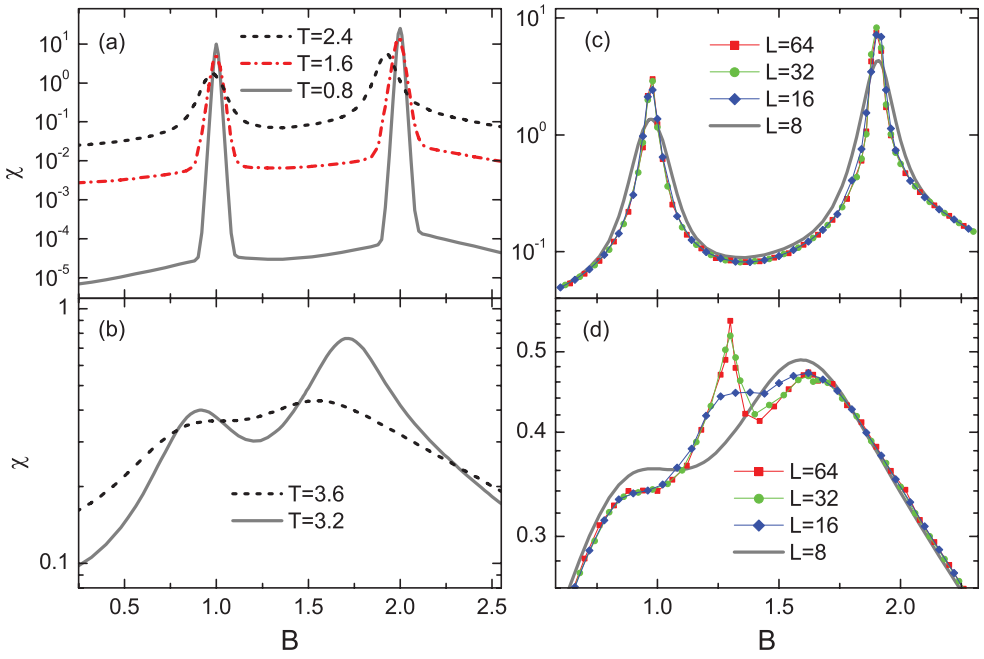

FIG. 6. (Color online) Susceptibility of thin films with eight layers as a function of magnetic field strength for various temperatures. (a),(b) Data derived from the density of states of a small system with 8×8 spins per layer. At low temperatures the phase transition is discontinuous, as revealed by the characteristic form of the peaks. Around $T \approx 2.2$ the form of the peaks changes, indicating that the transition has become continuous. (c) Susceptibility for $T = 2.5$ obtained for systems with different numbers of spins in the layers. Whereas the height of the peaks changes with system size, the location of the peaks does not show a dependence on the sizes of the layers. Symbols indicate data obtained using the Metropolis algorithm. (d) The same as in (c), but now for $T = 3.5$. For larger systems a critical peak, which indicates the transition to the paramagnetic phase, emerges that is not visible for the smallest systems. The peak at $B \approx 1.6$ is a noncritical peak. Error bars are comparable to the sizes of the symbols.

An interesting property of the phase diagram of thin metamagnetic films emerges when we study response functions at high temperatures and low fields. Whereas for low temperatures the response functions display a characteristic peak with a height that depends on the system size, for higher temperatures the response functions no longer display any dependence on the size of the system. As shown in Fig. 8 for the surface response functions, system-size-dependent peaks are no longer encountered in the ordered phase for temperatures $T \geqslant 2.50$ and fields $B \geqslant 0.98$. This excludes the existence of a line of continuous phase transitions at high temperatures and low fields, indicating that the line of discontinuous transitions

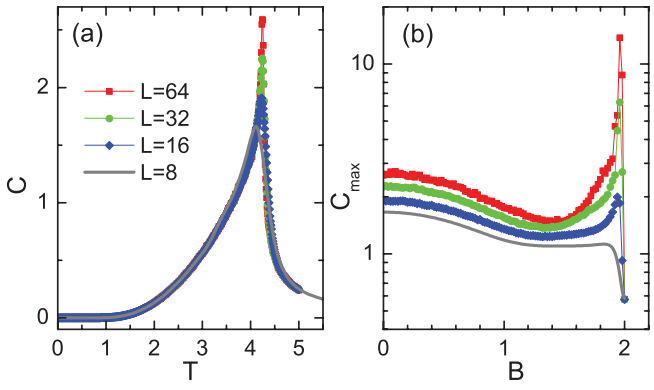

FIG. 7. (Color online) (a) Specific heat of an eight-layer system as a function of T for $B = 0$ and various sizes of the layers. The peaks indicate the transition between the ordered and paramagnetic phases. (b) The maximum height of the specific heat for a fixed value of the magnetic field strength B. This maximum value is achieved at the transition to the paramagnetic phase. The strong peak around $B \approx 1.96$ reveals the change of the order of the transition when the tricritical point is crossed.

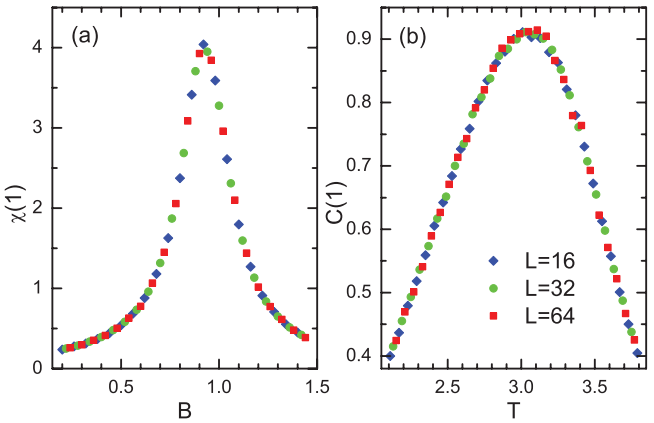

FIG. 8. (Color online) (a) Surface susceptibility (4) at $T = 3$ and (b) surface specific heat (5) at $B = 0.5$ for the surface layer that aligns with the magnetic field. Data obtained for different system sizes are shown. These maxima are noncritical and size independent, indicating that the reversal of the surface magnetization is gradual for these values of the system parameters.

ends in a critical end point. Therefore, instead of crossing a phase transition line, with its characteristic singularities, one can go from the antiferromagnetic phase at low temperatures and fields to the intermediate phase with one flipped layer in a smooth and gradual way. This is in complete analogy to the well-known behavior of water where one can go in a similar way from vapor to liquid without a phase transition. Based on our data, we locate this critical end point at $T = 2.50(5)$ and $B = 0.98(1)$.

IV. DISCUSSION AND CONCLUSION

The numerous possible applications have recently yielded a strong interest in artificial antiferromagnets and synthetic metamagnets. Remarkably, the layered structure of these materials allows for a high level of control of their physical properties through the fine-tuning of the strengths of both the inter- and intralayer interactions.

In order to get a better understanding of some of these properties, we presented a study of the equilibrium properties of thin Ising metamagnetic films. Indeed, neglecting the internal structure of ferromagnetic multilayers, one can model artificial antiferromagnets with strong perpendicular anisotropy by a layered Ising antiferromagnet. If one notes in addition that the synthetic metamagnets are usually composed of only a few repetitions of the superlattice structure, one is then naturally led to consider Ising metamagnets in thin film geometry.

Our work allowed us to study in detail the phase diagram of these systems as a function of temperature and of the strength of the applied external magnetic field. Earlier studies of related phenomenological models revealed[6,7] that for an even number of layers a layered antiferromagnet has three different $T = 0$ states, depending on the strength of the magnetic field. The antiferromagnetic structure, stable at low fields, goes over into a different ordered structure at intermediate field strengths. In this intermediate phase, one of the surface layers aligns with the direction of the magnetic field, the other layers remaining unchanged. At larger fields, the intermediate phase is replaced by the paramagnetic phase where all layers are parallel to the magnetic field. This intermediate phase is absent in the corresponding bulk system and is therefore characteristic for thin metamagnetic films.

Using the Wang-Landau algorithm and importance sampling Monte Carlo simulations, we thoroughly studied the equilibrium properties of our system. The Wang-Landau method yields the microcanonical entropy (or, alternatively, the degeneracy) as a function of magnetization and internal energy. The microcanonical entropy surface is rather complicated and reveals interesting features that we discussed in some detail. Thus we were able to relate the appearance of the intermediate phase to a subtle change in the microcanonical entropy when the boundary condition is changed.

Our canonical analysis of different thermal quantities, such as, for example, the global and layer magnetization, the global and layer susceptibility, and the global and layer specific heat, allows us to determine the temperature–magnetic field phase diagram shown in Fig. 5, which is the main result of our study. Interestingly, the discontinuous phase transition between the antiferromagnetic and the intermediate phases ends in a critical end point. It is therefore possible to pass from one phase to the other without undergoing a phase transition. Experimental studies on systems with strong perpendicular anisotropy should be able to verify this intriguing feature of thin Ising metamagnets.

As already mentioned in the Introduction, one of the motivations for our study was the recent investigation[33] of nonequilibrium relaxation and aging phenomena in Co/Cr superlattices. This study revealed intriguing nonequilibrium features that warrant a better understanding. As a first step in that direction, we started a study of the nonequilibrium properties of thin Ising metamagnets, but soon realized that a more complete understanding of the equilibrium properties of these systems is needed before being able to develop better insights into the more complex situation of relaxation far from equilibrium. With the knowledge of the equilibrium properties reported in this paper, we are now well prepared to better understand these complicated nonequilibrium processes. The results of this investigation will be the subject of a forthcoming presentation.

ACKNOWLEDGMENTS

We thank Christian Binek and Tatha Mukherjee for insightful discussions. This work was supported by the US National Science Foundation through Grant No. DMR-0904999. M.P. thanks the Max-Planck-Institut für Physik komplexer Systeme in Dresden, Germany, for hospitality during the completion of this work.

[1] E. E. Fullerton, D. T. Margulies, N. Supper, Do Hoa, M. Schabes, A. Berger, and A. Moser, IEEE Trans. Magn. **39**, 639 (2003).
[2] S. Mangin, D. Ravelosona, J. A. Katine, M. J. Carey, B. D. Terris, and E. E. Fullerton, Nat. Mater. **5**, 210 (2006).
[3] T. Mukherjee, S. Sahoo, R. Skomski, D. J. Sellmyer, and Ch. Binek, Phys. Rev. B **79**, 144406 (2009).
[4] O. Hellwig, T. L. Kirk, J. B. Kortright, A. Berger, and E. E. Fullerton, Nat. Mater. **2**, 112 (2003).
[5] O. Hellwig, A. Berger, J. B. Kortright, and E. E. Fullerton, J. Magn. Magn. Mater. **319**, 13 (2007).
[6] U. K. Rößler and A. N. Bogdanov, J. Magn. Magn. Mater. **269**, L287 (2004).
[7] U. K. Rößler and A. N. Bogdanov, Phys. Rev. B **69**, 094405 (2004).
[8] N. S. Kiselev, C. Bran, U. Wolff, L. Schultz, A. N. Bogdanov, O. Hellwig, V. Neu, and U. K. Rößler, Phys. Rev. B **81**, 054409 (2010).
[9] F. Harbus and H. E. Stanley, Phys. Rev. B **8**, 1141 (1973).
[10] J. M. Kincaid and E. G. D. Cohen, Phys. Rep. **22**, 57 (1975).
[11] D. P. Landau and R. H. Swendsen, Phys. Rev. Lett. **46**, 1437 (1981).
[12] H. J. Herrmann, E. B. Rasmussen, and D. P. Landau, J. Appl. Phys. **53**, 7994 (1982).

[13]D. P. Landau and R. H. Swendsen, Phys. Rev. B **33**, 7700 (1986).
[14]H. J. Herrmann and D. P. Landau, Phys. Rev. B **48**, 239 (1993).
[15]L. Hernández, H. T. Diep, and D. Bertrand, Europhys. Lett. **21**, 711 (1993).
[16]L. Hernández, H. T. Diep, and D. Bertrand, Phys. Rev. B **47**, 2602 (1993).
[17]W. Selke and S. Dasgupta, J. Magn. Magn. Mater. **147**, L245 (1995).
[18]S. Dasgupta, J. Stat. Phys. **81**, 837 (1995).
[19]W. Selke, Z. Phys. B **101**, 145 (1996).
[20]M. Pleimling and W. Selke, Phys. Rev. B **56**, 8855 (1997).
[21]S. Galam, C. S. O. Yokoi, and S. R. Salinas, Phys. Rev. B **57**, 8370 (1998).
[22]M. Santos and W. Figueiredo, Phys. Rev. B **58**, 9321 (1998).
[23]M. Žukovič and T. Idogaki, Phys. Rev. B **61**, 50 (2000).
[24]M. Santos and W. Figueiredo, Phys. Rev. E **62**, 1799 (2000).
[25]A. F. S. Moreira, W. Figueiredo, and V. B. Henriques, Eur. Phys. J. B **27**, 153 (2002).
[26]G. Gulpinar, D. Demirhan, and F. Buyukkilic, Physica A **383**, 372 (2007).
[27]J. Geng, G. Wei, and H. Miao, J. Magn. Magn. Mater. **320**, 1010 (2008).
[28]S. L. A. de Queiroz, Phys. Rev. E **80**, 041125 (2009)
[29]Y.-Q. Liang, G.-Z. Wei, X.-J. Xu, and G.-L. Song, J. Magn. Magn. Mater. **322**, 2219 (2010).
[30]B. Deviren and M. Keskin, Phys. Lett. A **374**, 3119 (2010).
[31]M. M. P. de Azevedo, Ch. Binek, J. Kushauer, W. Kleemann, and D. Bertrand, J. Magn. Magn. Mater. **140–144**, 1557 (1995).
[32]J. Pelloth, R. A. Brand, S. Takele, M. M. Pereira de Azevedo, W. Kleemann, Ch. Binek, J. Kushauer, and D. Bertrand, Phys. Rev. B **52**, 15372 (1995).
[33]T. Mukherjee, M. Pleimling, and Ch. Binek, Phys. Rev. B **82**, 134425 (2010).
[34]F. Wang and D. P. Landau, Phys. Rev. Lett. **86**, 2050 (2001).
[35]F. Wang and D. P. Landau, Phys. Rev. E **64**, 056101 (2001).
[36]D. H. E. Gross, *Microcanonical Thermodynamics: Phase Transitions in Small Systems*, Lecture Notes in Physics Vol. 66 (World Scientific, Singapore, 2001).
[37]M. Pleimling and H. Behringer, Phase Transitions **78**, 787 (2005).
[38]M. Kastner, M. Promberger, and A. Hüller, J. Stat. Phys. **99**, 1251 (2000).
[39]D. H. E. Gross and E. V. Votyakov, Eur. Phys. J. B **15**, 115 (2000).
[40]A. Hüller and M. Pleimling, Int. J. Mod. Phys. C **13**, 947 (2002).
[41]M. Pleimling, H. Behringer, and A. Hüller, Phys. Lett. A **328**, 432 (2004).
[42]J. Hove, Phys. Rev. E **70**, 056707 (2004).
[43]H. Behringer, M. Pleimling, and A. Hüller, J. Phys. A **38**, 973 (2005).
[44]A. Richter, M. Pleimling, and A. Hüller, Phys. Rev. E **71**, 056705 (2005).
[45]H. Behringer and M. Pleimling, Phys. Rev. E **74**, 011108 (2006).
[46]M. Kastner and M. Pleimling, Phys. Rev. Lett. **102**, 240604 (2009).
[47]C. Junghans, M. Bachmann, and W. Janke, Phys. Rev. Lett. **97**, 218103 (2006).
[48]M. Möddel, W. Janke, and M. Bachmann, Phys. Chem. Chem. Phys. **12**, 11548 (2010).
[49]M. N. Barber, in *Phase Transitions and Critical Phenomena* (Academic Press, London, 1983), Vol. 8, p. 145.
[50]Y. Li and K. Baberschke, Phys. Rev. Lett. **68**, 1208 (1992).
[51]P. Schilbe, S. Siebentritt, and K.-H. Rieder, Phys. Lett. A **216**, 20 (1996).
[52]R. Zhang and R. F. Willis, Phys. Rev. Lett. **86**, 2665 (2001).
[53]M. Pleimling, J. Phys. A **37**, R79 (2004).
[54]Ch. Binek, T. Kato, W. Kleemann, O. Petracic, D. Bertrand, F. Bourdarot, P. Burlet, H. Aruga Katori, K. Katsumata, K. Prokes, and S. Welzel, Eur. Phys. J. B **15**, 35 (2000).